Published for SISSA by Springer

Received: *October 3, 2020*
Accepted: *November 12, 2020*
Published: *December 23, 2020*

Addendum: Updated constraints on non-standard interactions from global analysis of oscillation data

Ivan Esteban,[a] **M.C. Gonzalez-Garcia,**[a,b,c] **Michele Maltoni,**[d] **Ivan Martinez-Soler**[d] **and Jordi Salvado**[a]

[a] *Departament de Fisíca Quàntica i Astrofísica and Institut de Ciencies del Cosmos, Universitat de Barcelona, Diagonal 647, E-08028 Barcelona, Spain*

[b] *Institució Catalana de Recerca i Estudis Avançats (ICREA), Pg. Lluis Companys 23, 08010 Barcelona, Spain*

[c] *C.N. Yang Institute for Theoretical Physics, State University of New York at Stony Brook, Stony Brook, NY 11794-3840, U.S.A.*

[d] *Instituto de Física Teórica UAM/CSIC, Universidad Autónoma de Madrid, Calle de Nicolás Cabrera 13–15, Cantoblanco, E-28049 Madrid, Spain*

E-mail: ivan.esteban@fqa.ub.edu, maria.gonzalez-garcia@stonybrook.edu, michele.maltoni@csic.es, ivanj.m@csic.es, jor.salvado@gmail.com

Addendum to: JHEP08(2018)180

ArXiv ePrint: 1805.04530

In this addendum we re-assess the constraints on Non-Standard Interactions (NSI) from the global analysis of neutrino oscillation data after including the new results released since the publication of ref. [1], in particular those presented at the Neutrino2020 conference. The new data considered here includes the total energy spectrum and the day-night asymmetry of the 2970-day SK4 solar neutrino sample [2], as well as the latest results from long-baseline (LBL) experiments T2K [3, 4] and NOvA [5, 6]. In addition, we have updated the reactor experiments Double-Chooz [7, 8] to 1276/587 days of far/near detector data and RENO [9, 10] to 2908 days of exposure.

The main effect driven by the new results concerns the analysis of solar and KamLAND data discussed in section 3 of ref. [1]. As explained there, at the time of publication there was a tension of $\Delta\chi^2 \sim 7.4$ between these two data sets within the context of the 3ν oscillation analysis, arising from a combination of two effects: (a) the ^{8}B measurements performed by SNO, SK and Borexino did not show any evidence of the low energy spectrum

https://doi.org/10.1007/JHEP12(2020)152

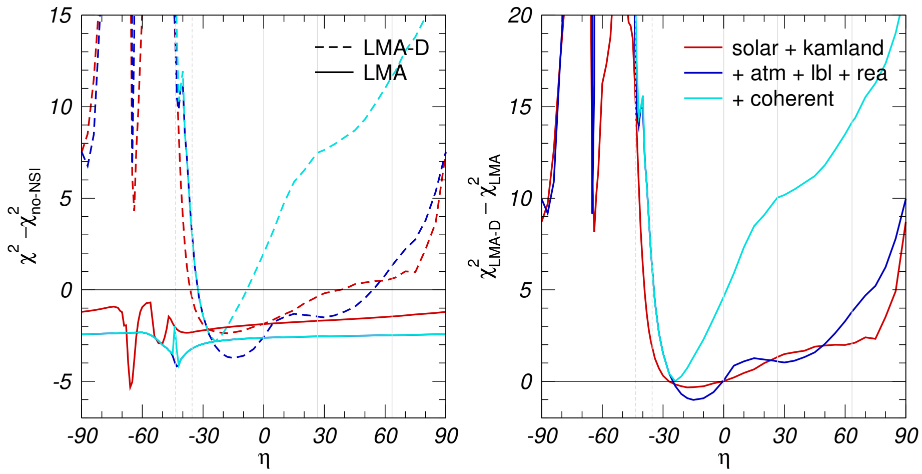

Figure 1. Left: $\chi^2_{\text{LMA}}(\eta) - \chi^2_{\text{no-NSI}}$ (full lines) and $\chi^2_{\text{LMA-D}}(\eta) - \chi^2_{\text{no-NSI}}$ (dashed lines) for the analysis of different data combinations (as labeled in the figure) as a function of the NSI quark coupling parameter η. The full dark blue and light blue curves lie on top of each other. Right: $\chi^2_{\text{dark}} - \chi^2_{\text{light}} \equiv \chi^2_{\text{LMA-D}}(\eta) - \chi^2_{\text{LMA}}(\eta)$ as a function of η. See text for details.

turn-up expected in the standard LMA-MSW [11, 12] solution for the value of Δm^2_{21} favored by KamLAND, and (b) the observation of a non-vanishing day-night asymmetry in SK, whose size was considerably larger than what predicted for the Δm^2_{21} value indicated by KamLAND. Such tension could be alleviated in presence of a non-standard matter potential, thus leading to a sizable decrease in the minimum χ^2 for the LMA solution for most values of η ($\Delta\chi^2 \sim -7 \to -11$), as could be observed in the left panel in figure 4 of ref. [1]. Correspondingly, in figure 2 of the same work, which showed the two-dimensional projections on the matter potential parameters $(\varepsilon_D^\eta, \varepsilon_N^\eta)$ of the 1σ, 90%, 2σ, 99% and 3σ CL (2 dof) allowed regions from the analysis of solar and KamLAND data in the presence of non-standard neutrino-matter interactions, the 3ν standard LMA oscillation scenario ($\varepsilon_D^\eta = \varepsilon_N^\eta = 0$) was outside of such allowed regions for most values of η.

As discussed in ref. [13], with the updated SK4 solar data the tension between the best fit Δm^2_{21} of KamLAND and that of the solar results has decreased to $\Delta\chi^2_{\text{solar}} = 1.3$. This is due to both the smaller day-night asymmetry, and the slightly more pronounced turn-up in the low energy part of the spectrum. So now in the left panel in figure 1 we see that for the LMA solution the fit with NSI leads to a decrease of about 1 unit of χ^2 for most values of η. Correspondingly in figure 2 the 3ν standard LMA oscillation scenario, $\varepsilon_D^\eta = \varepsilon_N^\eta = 0$ lies inside the 1σ LMA allowed regions for most values of η. Concerning the status of the LMA-D solution, the right panel in figure 1 shows that now LMA-D is allowed below 3σ for $\eta > -40°$ in the analysis of solar+KamLAND, for $-38° \lesssim \eta \lesssim 87°$ in the global oscillation analysis, and for $-38° \lesssim \eta \lesssim 20°$ when including information from the total event rate at COHERENT.[1] From the left panel we read that the best fit for the global analysis of

[1]We remind the reader that, as discussed in section 5 of ref. [1], while oscillation constraints apply to models where NSI are generated by arbitrarily light mediators, there is a minimum mediator mass for which the bounds of COHERENT are relevant, which we estimate to be $\mathcal{O}(10\text{–}50)$ MeV (see also refs. [14, 15]).

JHEP12(2020)152

JHEP12(2020)152

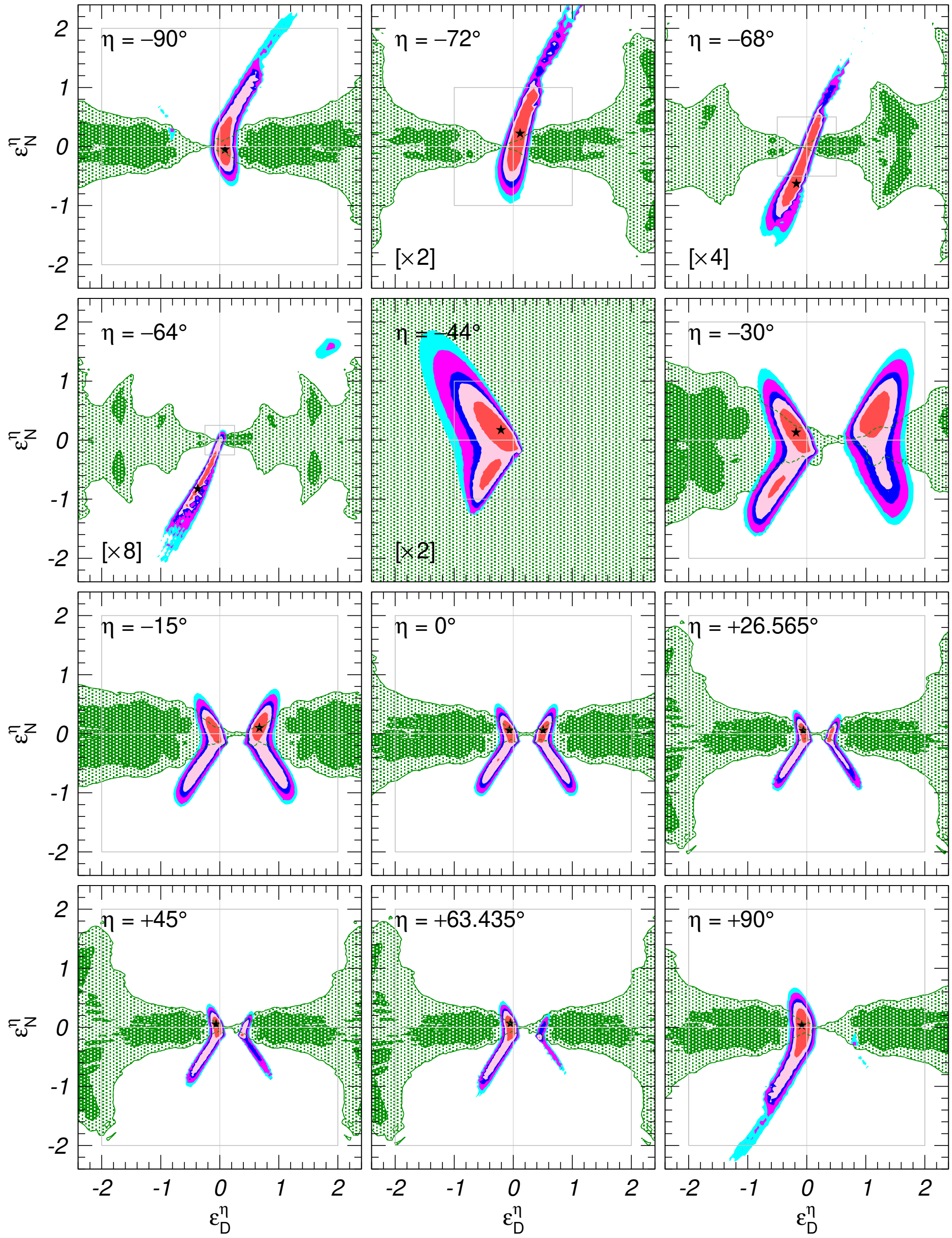

Figure 2. Two-dimensional projections of the 1σ, 90%, 2σ, 99% and 3σ CL (2 dof) allowed regions from the analysis of solar and KamLAND data in the presence of non-standard matter potential for the matter potential parameters $(\varepsilon_D^\eta, \varepsilon_N^\eta)$, for $\sin^2\theta_{13} = 0.022$ and after marginalizing over the oscillation parameters. The best fit point is marked with a star. The results are shown for fixed values of the NSI quark coupling parameter η. The panels with a scale factor "$[\times N]$" in their lower-left corner have been "zoomed-out" by such factor with respect to the standard axis ranges, hence the grey square drawn in each panel always corresponds to $\max\left(|\varepsilon_D^\eta|, |\varepsilon_N^\eta|\right) = 2$ and has the same size in all the panels. For illustration we also show as shaded green areas the 90% and 3σ CL allowed regions from the analysis of the atmospheric and LBL data. Note that, as a consequence of the periodicity of η, the regions in the first ($\eta = -90°$) and last ($\eta = +90°$) panels are identical up to an overall sign flip.

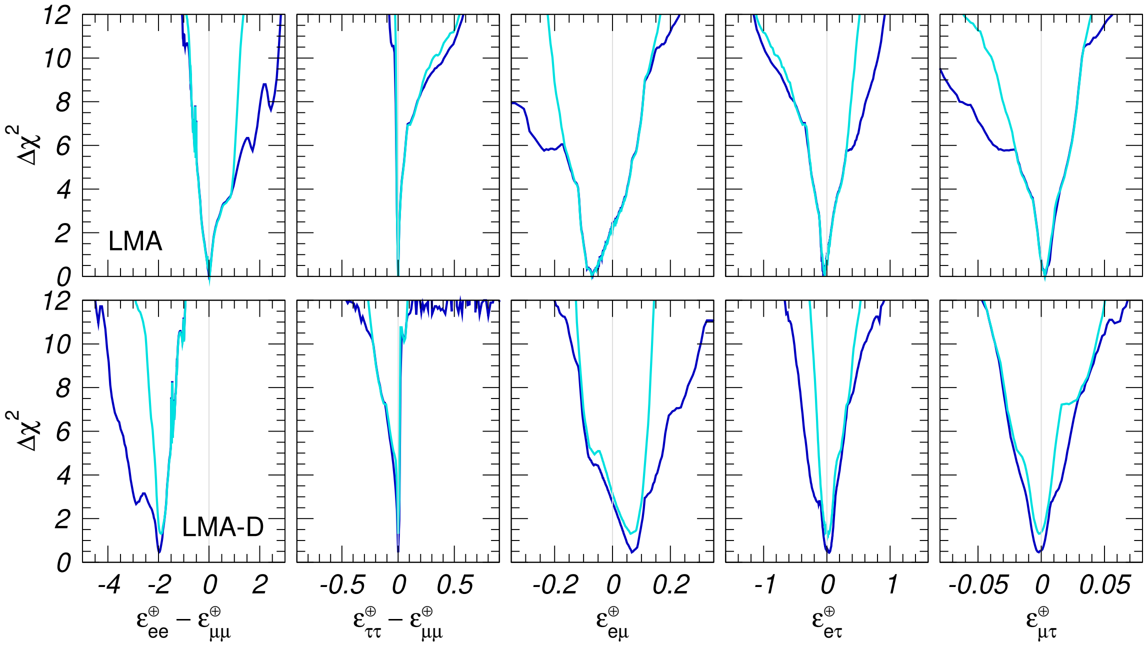

Figure 3. Dependence of the $\Delta\chi^2$ function on the effective NSI parameters relevant for matter effects in LBL experiments with arbitrary values of η, from the global analysis of solar, atmospheric, LBL-CPC and reactor data (blue lines) and including also COHERENT (cyan lines). The upper (lower) panels correspond to solutions within the LMA (LMA-D) subset of parameter space.

oscillations and also in combination with COHERENT corresponds to $\eta \sim -45°$ for LMA. For LMA-D the best fit for OSC (OSC+COH) is obtained for $\eta \sim -15°$ ($\eta \sim -20°$).

In figure 3 we plot the dependence of the global χ^2 on each NSI effective coupling relevant for neutrino propagation in the Earth after marginalization over all other parameters including η, so that the $\Delta\chi^2$ functions plotted in the figure are defined with respect to the absolute minimum for any η. When compared with the corresponding figure in ref. [1] we observe that, following the discussion above, the minimum χ^2 within LMA and LMA-D are almost the same, while previously we had $\Delta\chi^2_{\text{min,LMA-D}} \sim 3$. The other observable difference is that including COHERENT has now a larger impact on the allowed ranges in LMA.

Finally, for the sake of convenience and comparison with previous results we list in the first columns in table 1 the 95% CL ranges for NSI with up-quarks only, down-quarks only, and protons. Generically the allowed ranges with in LMA are slightly reduced and, as expected, the allowed ranges for $\varepsilon_{ee} - \varepsilon_{\mu\mu}$ are now more symmetric around zero.

Acknowledgments

This work was supported by the spanish grants FPA2016-76005-C2-1-P, FPA2016-78645-P, PID2019-105614GB-C21 and PID2019-110058GB-C21, by USA-NSF grant PHY-1915093, by AGAUR (Generalitat de Catalunya) grant 2017-SGR-929, by EU ITN project H2020-MSCA-ITN-2019/870881-HIDDeN, and by the Spanish Agencia Estatal de Investigación through the grant "IFT Centro de Excelencia Severo Ochoa SEV-2016-0597". Fermilab is

OSC			+ COHERENT	
	LMA	LMA $\oplus$ LMA-D		LMA = LMA $\oplus$ LMA-D
$\varepsilon^u_{ee} - \varepsilon^u_{\mu\mu}$	$[-0.072, +0.321]$	$\oplus[-1.042, -0.743]$	ε^u_{ee}	$[-0.067, +0.547]$
$\varepsilon^u_{\tau\tau} - \varepsilon^u_{\mu\mu}$	$[-0.001, +0.018]$	$[-0.016, +0.018]$	$\varepsilon^u_{\mu\mu}$	$[-0.076, +0.455]$
			$\varepsilon^u_{\tau\tau}$	$[-0.076, +0.455]$
$\varepsilon^u_{e\mu}$	$[-0.050, +0.020]$	$[-0.050, +0.059]$	$\varepsilon^u_{e\mu}$	$[-0.050, +0.020]$
$\varepsilon^u_{e\tau}$	$[-0.077, +0.098]$	$[-0.111, +0.098]$	$\varepsilon^u_{e\tau}$	$[-0.077, +0.099]$
$\varepsilon^u_{\mu\tau}$	$[-0.006, +0.007]$	$[-0.006, +0.007]$	$\varepsilon^u_{\mu\tau}$	$[-0.006, +0.007]$
$\varepsilon^d_{ee} - \varepsilon^d_{\mu\mu}$	$[-0.084, +0.326]$	$\oplus[-1.081, -1.026]$	ε^d_{ee}	$[-0.063, +0.503]$
$\varepsilon^d_{\tau\tau} - \varepsilon^d_{\mu\mu}$	$[-0.001, +0.018]$	$[-0.001, +0.018]$	$\varepsilon^d_{\mu\mu}$	$[-0.072, +0.408]$
			$\varepsilon^d_{\tau\tau}$	$[-0.072, +0.407]$
$\varepsilon^d_{e\mu}$	$[-0.051, +0.020]$	$[-0.051, +0.038]$	$\varepsilon^d_{e\mu}$	$[-0.050, +0.020]$
$\varepsilon^d_{e\tau}$	$[-0.077, +0.098]$	$[-0.077, -0.098]$	$\varepsilon^d_{e\tau}$	$[-0.078, +0.098]$
$\varepsilon^d_{\mu\tau}$	$[-0.006, +0.007]$	$[-0.006, +0.007]$	$\varepsilon^d_{\mu\tau}$	$[-0.006, +0.007]$
$\varepsilon^p_{ee} - \varepsilon^p_{\mu\mu}$	$[-0.190, +0.927]$	$\oplus[-2.927, -1.814]$	ε^p_{ee}	$[-0.222, +1.801]$
$\varepsilon^p_{\tau\tau} - \varepsilon^p_{\mu\mu}$	$[-0.001, +0.053]$	$[-0.052, +0.053]$	$\varepsilon^p_{\mu\mu}$	$[-0.248, +0.282] \oplus [+0.625, +1.551]$
			$\varepsilon^p_{\tau\tau}$	$[-0.248, +0.281] \oplus [+0.646, +1.548]$
$\varepsilon^p_{e\mu}$	$[-0.145, +0.058]$	$[-0.145, +0.145]$	$\varepsilon^p_{e\mu}$	$[-0.145, +0.058]$
$\varepsilon^p_{e\tau}$	$[-0.238, +0.292]$	$[-0.292, +0.292]$	$\varepsilon^p_{e\tau}$	$[-0.239, +0.293]$
$\varepsilon^p_{\mu\tau}$	$[-0.019, +0.021]$	$[-0.021, +0.021]$	$\varepsilon^p_{\mu\tau}$	$[-0.019, +0.021]$

Table 1. 2σ allowed ranges for the NSI couplings $\varepsilon^u_{\alpha\beta}$, $\varepsilon^d_{\alpha\beta}$ and $\varepsilon^p_{\alpha\beta}$ as obtained from the global analysis of oscillation data (left column) and also including COHERENT constraints. The results are obtained after marginalizing over oscillation and the other matter potential parameters either within the LMA only and within both LMA and LMA-D subspaces respectively (this second case is denoted as LMA $\oplus$ LMA-D). Notice that once COHERENT data are included the two columns become identical in all cases since for NSI couplings to $f = u, d, p$ the LMA-D solution is only allowed above 95% CL.

operated by the Fermi Research Alliance, LLC under contract No. DE-AC02-07CH11359 with the United States Department of Energy. IE acknowledges support from the FPU program fellowship FPU15/0369. IMS acknowledge travel support from the Colegio de Fisica Fundamental e Interdisciplinaria de las Americas (COFI). The authors acknowledge use of the HPC facilities at the IFT (Hydra cluster).

JHEP12(2020)152

References

[1] I. Esteban, M.C. Gonzalez-Garcia, M. Maltoni, I. Martinez-Soler and J. Salvado, *Updated Constraints on Non-Standard Interactions from Global Analysis of Oscillation Data*, *JHEP* **08** (2018) 180 [arXiv:1805.04530] [INSPIRE].

[2] Y. Nakajima, *SuperKamiokande*, talk given at the *XXIX International Conference on Neutrino Physics and Astrophysics*, Chicago, U.S.A., June 22–July 2, 2020 (online conference) [DOI].

[3] T2K collaboration, *Constraint on the matter-antimatter symmetry-violating phase in neutrino oscillations*, *Nature* **580** (2020) 339 [*Erratum ibid.* **583** (2020) E16] [arXiv:1910.03887] [INSPIRE].

[4] P. Dunne, *Latest Neutrino Oscillation Results from T2K*, talk given at the *XXIX International Conference on Neutrino Physics and Astrophysics*, Chicago, U.S.A., June 22–July 2, 2020 (online conference) [DOI].

[5] NOvA collaboration, *First Measurement of Neutrino Oscillation Parameters using Neutrinos and Antineutrinos by NOvA*, *Phys. Rev. Lett.* **123** (2019) 151803 [arXiv:1906.04907] [INSPIRE].

[6] A. Himmel, *New Oscillation Results from the NOvA Experiment*, talk given at the *XXIX International Conference on Neutrino Physics and Astrophysics*, Chicago, U.S.A., June 22–July 2, 2020 (online conference) [DOI].

[7] Double CHOOZ collaboration, *Double CHOOZ θ_{13} measurement via total neutron capture detection*, *Nature Phys.* **16** (2020) 558 [arXiv:1901.09445] [INSPIRE].

[8] T. Bezerra, *New Results from the Double Chooz Experiment*, talk given at the *XXIX International Conference on Neutrino Physics and Astrophysics*, Chicago, U.S.A., June 22–July 2, 2020 (online conference) [DOI].

[9] RENO collaboration, *Measurement of Reactor Antineutrino Oscillation Amplitude and Frequency at RENO*, *Phys. Rev. Lett.* **121** (2018) 201801 [arXiv:1806.00248] [INSPIRE].

[10] J. Yoo, *RENO*, talk given at the *XXIX International Conference on Neutrino Physics and Astrophysics*, Chicago, U.S.A., June 22–July 2, 2020 (online conference) [DOI].

[11] L. Wolfenstein, *Neutrino Oscillations in Matter*, *Phys. Rev. D* **17** (1978) 2369 [INSPIRE].

[12] S.P. Mikheyev and A. Smirnov, *Resonance Amplification of Oscillations in Matter and Spectroscopy of Solar Neutrinos*, *Sov. J. Nucl. Phys.* **42** (1985) 913 [INSPIRE].

[13] I. Esteban, M.C. Gonzalez-Garcia, M. Maltoni, T. Schwetz and A. Zhou, *The fate of hints: updated global analysis of three-flavor neutrino oscillations*, *JHEP* **09** (2020) 178 [arXiv:2007.14792] [INSPIRE].

[14] P.B. Denton, Y. Farzan and I.M. Shoemaker, *Testing large non-standard neutrino interactions with arbitrary mediator mass after COHERENT data*, *JHEP* **07** (2018) 037 [arXiv:1804.03660] [INSPIRE].

[15] P. Coloma, M.C. Gonzalez-Garcia and M. Maltoni, *Neutrino Oscillation Constraints on* U(1)′ *Models: from Non-Standard Interactions to Long-Range Forces*, arXiv:2009.14220 [INSPIRE].

JHEP12(2020)152